

Correlation Between Luminosity and Accretion Torque in 4U 1626–67 and GX 301–2

Brian A. Vaughan¹ and Shunji Kitamoto^{2,3}

ABSTRACT

We present X-ray light curves and energy spectra for the persistent accreting pulsars 4U 1626–67 and GX 301–2 measured by the All-Sky Monitor (ASM) on *Ginga* from 1987 March – 1991 October. We compare these with simultaneous and near simultaneous measurements of spin frequency and flux by other instruments, principally the Burst and Transient Source Experiment (BATSE) on the Compton Gamma Ray Observatory (CGRO). A dramatic change in the shape of the X-ray spectrum and a $\sim 20\%$ decrease in the 1–20 keV X-ray flux accompany the 1990 transition from steady spin up to steady spin down in 4U 1626–67. The *Ginga* ASM is the only instrument to observe 4U 1626–67 during both spin up and spin down. We show that the distance to 4U 1626–67 is $\gtrsim 5$ kpc. If 4U 1626–67 is a near-equilibrium rotator and if the 0.04 Hz Quasi-Period Oscillations seen during spin up are magnetospheric beat-frequency oscillations, then the distance to the source is ~ 5 kpc, assuming a neutron-star mass of $1.4 M_{\odot}$, radius 10 km, and moment of inertia 10^{45} g cm².

The X-ray flux of GX 301–2 measured with the ASM varies with orbital phase. The flux peaks shortly before periastron, with a secondary maximum near apastron. Such variations were seen previously in the 20–50 keV pulsed flux with BATSE. The ASM observations confirm that the 20–50 keV pulsed flux in GX 301–2 is a good tracer of the bolometric flux. The X-ray flux in GX 301–2 was a factor of ~ 2 larger than average during the periastron passage prior to an episode of persistent spin up in 1991 July observed with BATSE that lasted half an orbit and resembled outbursts seen in transient X-ray pulsars. No ASM observations were available during the spin-up episode.

Subject headings: Stars: Binaries: General — Stars: Neutron — Accretion, Accretion Disks — Stars: Pulsars — X-rays: Stars — Stars: Individual (4U1626-67, GX301-2)

1. Introduction

Accreting pulsars consist of rotating, magnetized neutron stars that accrete matter from a companion (Pringle & Rees 1972; Davidson & Ostriker 1971). Material may be captured either from the stellar wind of the companion (wind accretion) or through Roche-lobe overflow of the mass donating star (disk accretion). The flow of material, either radially inward or through an accretion disk, is interrupted when magnetic stresses dominate material stresses at the magnetospheric radius, $r_m = K \mu^{4/7} (GM_x)^{-1/7} \dot{M}^{-2/7}$. Here, μ is

¹Space Radiation Laboratory, California Institute of Technology, MC 220–47, Pasadena CA 91125; brian@srl.caltech.edu

²Department of Earth and Space Science, Graduate School of Science, Osaka University 1–1, Machikaneyama-cho, Toyonaka, Osaka, 560, Japan; kitamoto@ess.sci.osaka-u.ac.jp

³CREST, Japan Science and Technology Corporation (JST)

the neutron-star magnetic moment, M_x is its mass, \dot{M} is the mass accretion rate, and K is a constant of order unity. For $K = 0.91$, R_m is equal to the Alfvén radius for spherical accretion.

In the simplest picture of disk accretion, matter becomes attached to magnetic field lines at r_m and transported to the magnetic poles. If the angular momentum of material captured from the disk at r_m is carried to the neutron star, the neutron star experiences an accretion torque

$$N = \dot{M} \sqrt{GM_x r_m}. \quad (1)$$

A star with moment of inertia I_x subject to the torque in equation (1) will spin up at a rate

$$2\pi I_x \dot{\nu} = (GM_x)^{3/7} \mu^{2/7} \dot{M}^{6/7}. \quad (2)$$

Assuming the gravitational potential energy of the accreted material is converted to X-rays at the neutron-star surface, the X-ray luminosity will be

$$L_x \approx G\dot{M}M_x/r_x, \quad (3)$$

where r_x is the neutron-star radius. From equations (2) and (3), the rate of spin up is related to the X-ray intensity through $\dot{\nu} \propto L_x^{6/7}$.

If the magnetospheric radius lies outside the corotation radius, r_{co} , where the Keplerian orbital frequency equals the spin frequency of the neutron star, matter that becomes attached to field lines may be expelled from the system. Accretion is then centrifugally inhibited. In this “propellor” regime, the neutron star may spin down rapidly. Neutron stars accreting at a constant rate thus tend toward an equilibrium spin period where $r_m \approx r_{co}$, given by

$$P_{eq} = 2\pi(GM_x)^{-5/7} \mu^{6/7} \dot{M}^{-3/7}. \quad (4)$$

The relation between torque and luminosity near equilibrium is expected to be more complicated than equation (1).

Magnetic accretion occurs in a variety of astrophysical systems, including magnetic CVs and T Tauri stars (Warner 1990; Konigl et al. 1991). Accreting pulsars are well suited for studying accretion phenomena. Their small moments of inertia and strong magnetic fields result in measureable changes in the spin frequency, ν , in hours to days with current instruments (e.g. Nagase 1989). In particular, accreting pulsars open the possibility of probing the interaction between material in the accretion disk and the magnetic field through measurements of how $\dot{\nu}$ depends upon \dot{M} .

A correlation between spin-up rate and X-ray luminosity has been observed in outbursts of 5 transient systems; between the spin-up rate and the 1–20 keV flux measured with EXOSAT in EXO 2030+375 (Parmar, White & Stella 1989; Parmar et al. 1989; Reynolds et al. 1996), and between the spin-up rate and the flux above 20 keV (in some cases the pulsed flux) measured with BATSE in 2S 1417–62 (Finger, Wilson & Chakrabarty 1996), A 0535+26 (Bildsten et al. 1997; Finger, Wilson & Harmon 1996), GS 0834-43 (Wilson et al. 1997) and GRO J1744–28 (Bildsten et al. 1997). All of these outbursts had luminosities and accretion torques exceeding those normally observed in most persistent sources. They almost certainly satisfy $r_m \ll r_{co}$ during most of the outburst.

The case for torque-luminosity correlations in persistent sources is less clear. The disk-fed systems Cen X-3 and GX 1+4 both exhibit strong flares lasting several days. In Cen X-3, no correlation between the pulse frequency history and the X-ray flux history has been found (Tsunemi, Kitamoto & Tamura 1996; Bildsten et al. 1997). In GX 1+4, there is an *anticorrelation* between the 20–50 keV pulsed flux measured with the BATSE and accretion torque (Chakrabarty et al. 1997b). In the wind-fed system GX 301–2, the X-ray flux has been found to vary with orbital phase. However, continuous measurements with BATSE show no correlation between orbital phase and either the magnitude or the sense of the accretion torque (Koh et al. 1997).

In this paper we present measurements of X-ray flux for the accreting pulsars 4U 1626–67 and GX 301–2 made with the All-Sky Monitor (ASM) on the *Ginga* satellite over the course of 4.5 years. We describe the ASM in Section 2. Although the “snapshots” of source flux taken by the ASM cannot be used to determine the frequency histories of pulsed sources, they are a long term, uniform set of measurements that can be correlated with other measurements. In particular, they complement measurements of pulse frequency made with BATSE, whose low-energy cutoff of ~ 20 keV misses most of the bolometric luminosity of most pulsars, a point we return to in the discussion. The two instruments overlapped from 1991 April–October.

4U 1626–67 is a low-mass, disk-fed accreting pulsar with a 7.6 s spin period, a 42 minute orbital period (Middleditch et al. 1981; Chakrabarty et al. 1997a), and a low-mass ($M < 0.1M_{\odot}$) helium or carbon-oxygen dwarf companion KZ Tra (Levine et al. 1988). 4U 1626–67 was observed to be in a state of steady spin up at a rate of $\dot{\nu} \sim 8.5 \times 10^{-13} \text{ Hz s}^{-1}$ for nearly two decades since its discovery by *Uhuru* in 1972. Observations with BATSE have shown it to be in a state of spin down at a rate of $\dot{\nu} \sim -7.2 \times 10^{-13} \text{ Hz s}^{-1}$ since 1991. Quasi-Periodic oscillations in X-ray intensity with a frequency of 0.04 Hz were observed during spin up (Shinoda et al. 1990). During spin down, the QPO frequency was 0.048 Hz (Angelini et al. 1995).

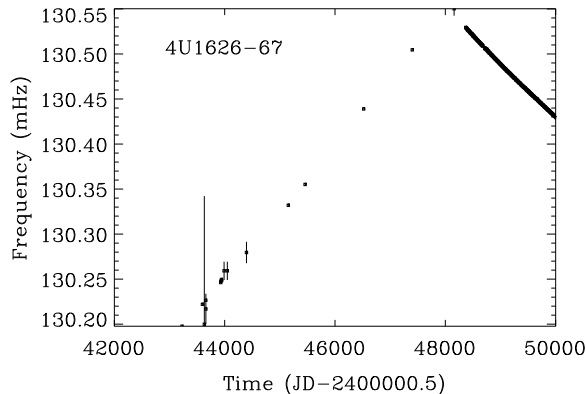


Fig. 1.— The frequency history of 4U 1626–67 since 1972.

Figure 1 shows the frequency history of 4U 1626–67. Extrapolating the spin-up trend observed from 1975 through 1988 (Levine et al. 1988) and the spin-down trend observed by BATSE from 1991 through the present (Chakrabarty et al. 1997a) yields a transition from spin-up to spin-down in mid 1990. We note that both the spin-up and spin-down trends have significant higher-order components (Levine et al. 1988; Chakrabarty 1997a), hence the transition time is approximate. The rate of spin-down shortly after the turnaround, as measured with BATSE, is roughly 15% slower than the rate of spin up prior to the turnaround as measured by previous instruments.

GX 301-2 is a high-mass, wind fed accreting pulsar with a 680s spin period, a highly-eccentric ($e = 0.47$) 42 day orbit, and a high-mass ($M \geq 40M_{\odot}$) OB supergiant companion Wray 977 (Koh et al. 1997). Daily BATSE spin-frequency measurements show that most of the time, GX 301-2 experiences a rapidly-changing accretion torque with virtually no net change in spin frequency on long time scales. However, BATSE observed two episodes of steady, rapid spin up from MJD 48440–48463 (orbital phase $\phi = 0.25 - 0.8$), and MJD 49230–49245 ($\phi = 0.3 - 0.65$), with an average spin-up rate of $4.5 \times 10^{-12} \text{ Hz s}^{-1}$. The pulsed flux in 20–55 keV during the spin-up episodes is $1.9 \times 10^{-9} \text{ erg cm}^{-2} \text{ s}^{-1}$, 50% higher than the average pulsed flux for the same orbital phase, and almost twice as high as the average pulsed flux over all orbital phases (Koh et al. 1997). The pulsed flux measured with BATSE depends strongly on orbital phase, with a peak slightly before periastron and a secondary peak at apastron.

2. Observations

The *Ginga* ASM performed well throughout the 1987 February to 1991 October period that *Ginga* was in orbit. The effective area of the ASM was about 420 cm^2 , with a $45^{\circ} \times 1^{\circ}$ FWHM fan-beam collimator. Details of the ASM appear in Tsunemi et al. (1989). Sky-scanning observations with the ASM were typically performed at intervals of a few days, when the satellite was rotated around the z -axis in 20 min. During such scanning observations, 16-channel source spectra were obtained covering the energy range 1 to 20 keV. An exposure time of 3–18s was obtained for each scan across each observed source, depending on the source’s latitude in the spacecraft equatorial (xy) plane. For favorably located sources, the detection limit was about 50 mCrab (1–6 keV), at the 5σ level, worsening for sources far from the spacecraft equatorial plane.

Data selection criteria included: (1) background low and stable, (2) source unocculted by the Earth, and (3) acceptable spacecraft aspect, such that the source was within 25° of the center of the ASM field of view. During the 4.5 year mission, a total of 294 observations of 4U 1626–67 and 277 observations of GX 301–2 satisfied these conditions and were accepted for follow-on analysis.

In the discussion we make extensive use of frequencies and pulsed fluxes measured with BATSE. BATSE consists of 8 uncollimated detector modules facing outward from the corners of the CGRO spacecraft. Each of the 8 modules contains a Large Area Detector with a $2\pi\text{Sr}$ field of view, sensitive to photons with energies of 20–1800 keV. Fluxes measured with BATSE suffer from the limitation that the bulk of the bolometric flux from most accreting pulsars is in the energy range 1–20 keV. Further, the background is large and variable. Only the pulsed component of the flux can be measured by epoch folding BATSE data. BATSE observations of accreting pulsars are discussed in detail in Bildsten et al. (1997).

3. Results

3.1. 4U 1626–67

Ginga ASM light curves of 4U 1626–67 in 1–6 keV and 6–20 keV are plotted in Figure 2. Each point is the average of 30 d (typically ~ 10 pointings). The 1–6 keV count rate shows a clear drop in mid 1990. The average counting rate in 1–6 keV is $0.0443(18) \text{ cm}^{-2} \text{ s}^{-1}$ from 1987 February – 1990 May, and $0.0124(37) \text{ cm}^{-2} \text{ s}^{-1}$ from 1990 June – 1991 November. In 6–20 keV, the average rate is $0.0295(17) \text{ cm}^{-2} \text{ s}^{-1}$ from 1987 February – 1990 May, and $0.0176(29) \text{ cm}^{-2} \text{ s}^{-1}$ from 1990 June – 1991 November. Count-rate

variations are consistent with measurement errors within both intervals. Thus, the 1–6 keV count rate is smaller after 1990 June than before 1990 June by 72%, and the 6–20 keV count rate by 40%.

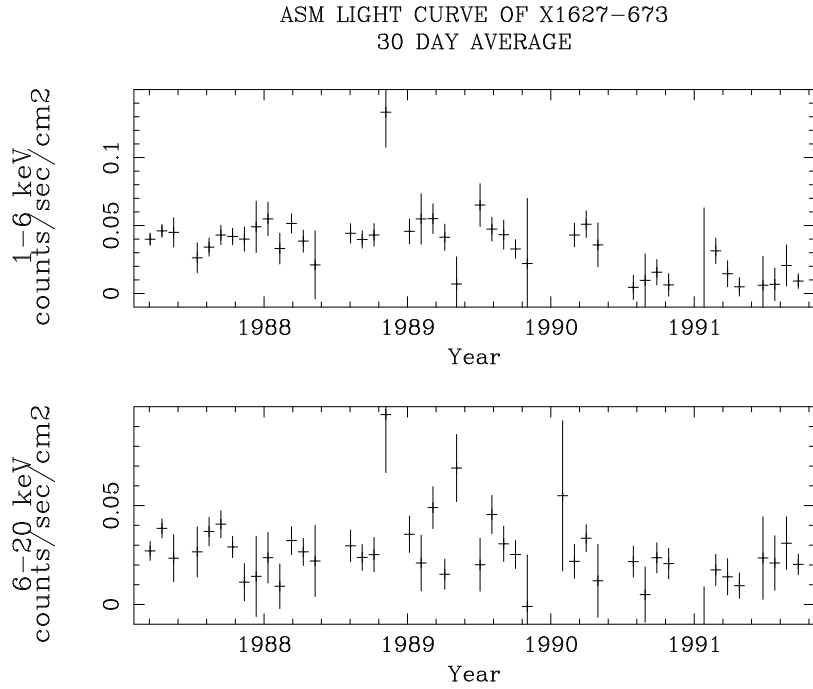


Fig. 2.— The 4.5 year flux history of 4U 1626–67 observed with the *Ginga* ASM. Each datum is an average over 30 days.

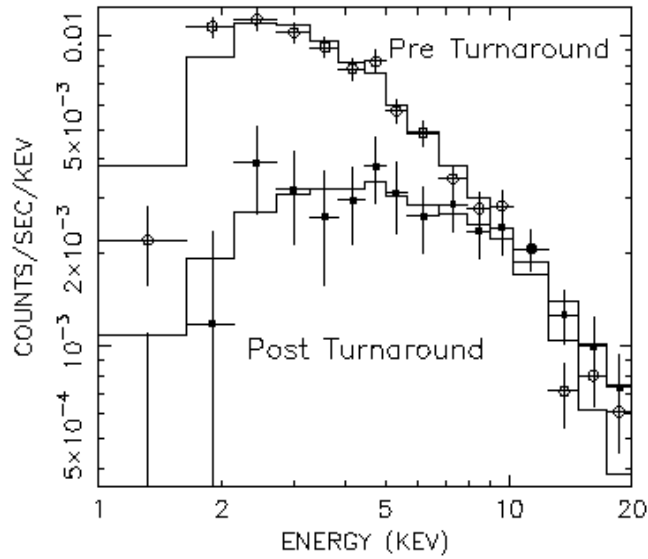


Fig. 3.— Two average energy spectra of 4U 1626–67 obtained by *Ginga* ASM observation. The open circles

give the average spectrum before turnaround, and filled circles give the average spectrum after turnaround. The histograms are best-fit power law models.

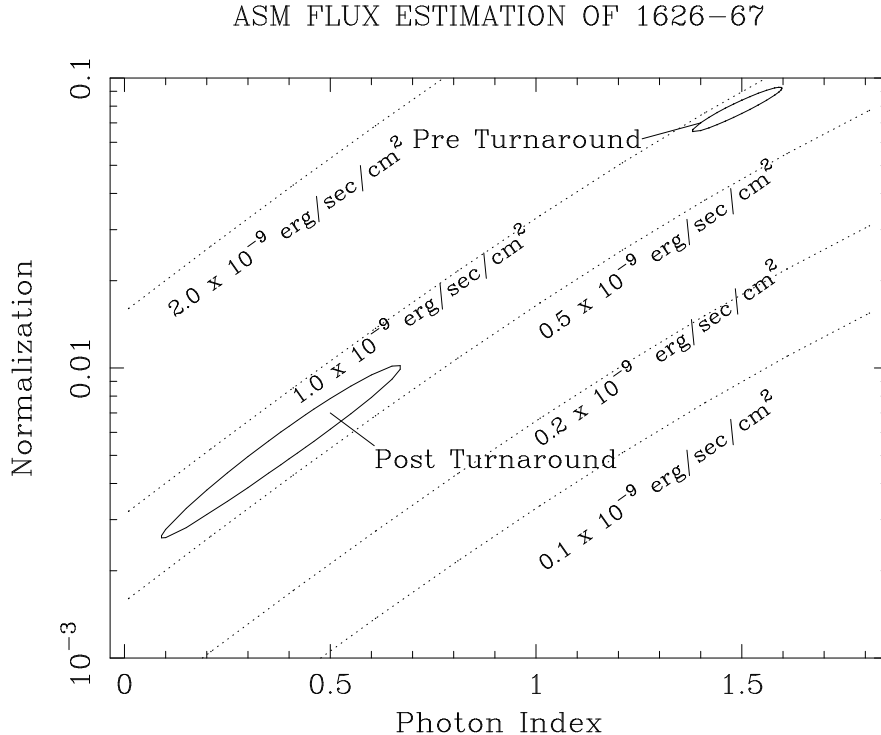


Fig. 4.— Confidence contours (90% for 4U 1626–67). Dotted lines indicate constant flux contours.

Figure 3 shows the average energy spectrum of 4U 1626–67 before and after 1990 June. We fit both spectra by a simple power law model; $N(E) = AE^{-\alpha}$. Previous instruments have found the column density to be negligible. We verified that $N_{\text{H}} \leq 10^{21} \text{ cm}^{-2}$ using data obtained before and after the turnaround, then fixed the column density at zero. The 90% confidence contours of the best fit parameters are shown in Figure 4. The pre-1990 June photon spectrum can be fit with $A = 0.078(7) \text{ cm}^{-2} \text{ s}^{-1} \text{ keV}^{-1}$ (at 1 keV) and $\alpha = 1.48(5)$. The post-June 1990 spectrum can also be fit using a power law with $A = 0.006(3) \text{ cm}^{-2} \text{ s}^{-1} \text{ keV}^{-1}$ and $\alpha = 0.41(22)$. In Figure 4, lines of constant 1–20 keV flux, F_x are plotted as dotted lines. The flux before 1990 June is slightly higher than after. The flux in 1–10 keV, 10–20 keV and 1–20 keV are given in Table 1 for pre- and post-1990 June spectra. The 1–10 keV flux is observed to drop by more than 50%, and the 1–20 keV flux by roughly 20%. The decrease in flux is less than the decrease in count rate because the spectrum during spin down is harder.

Chakrabarty et al. (1997a) have compared the spectra of 4U 1626–67 measured with a variety of instruments including HEAO1, Einstein, *Ginga* LAC, and ASCA. The photon spectral index of 0.41 measured with the *Ginga* ASM after turnaround is the smallest ever measured for this source. To evaluate the possibility that absorption or scattering of low energy photons is responsible for the change in spectrum, we fixed the power-law spectral index at the pre turnaround value and attempted to fit the post turnaround

Table 1: 4U 1626–67 X-ray Flux

Bandpass	Spin-up Flux ¹	Spin-down Flux ¹
	1987 Mar.–1990 May	1990 Jun.–1991 Oct.
1–20 keV	8.89±0.56	6.67±0.89
1–10 keV	5.49±0.32	2.15±0.45
10–20 keV	3.39±0.45	4.48±0.80

¹ 10^{-10} erg cm⁻² s⁻¹

spectrum by varying the absorption. This did not yield an acceptable fit, and a large excess below 3 keV appears in residuals. A partial covering model coupled with a power law did provide a reasonable fit, where 86(6)% of the X-rays are obscured by thick material with a column density of $10^{23.8(2)}$ cm⁻², and the remaining X-rays are unabsorbed ($n_H < 10^{21}$ cm⁻²). If this partial covering model is correct, the 1–20 keV flux, F_x , is 1.65(47) times larger during spin down than during spin-up.

3.2. GX 301-2

Ginga ASM light curves of GX 301–2 in 1–6 and 6–20 keV are plotted in Figure 5. Each point corresponds to one scanning observation. Since the duration of each observation (3–18 s) is shorter than the spin period of GX 301–2 (~680 s), the count rate depends upon the pulse phase at the time of the observation, which introduces scatter into the measurements.

The first of the two episodes of rapid spin up observed with BATSE occurred during *Ginga* operation. Unfortunately, the *Ginga* ASM did not observe GX 301–2 during the spin-up episode. However, the periastron passage prior to spin up is well covered. The average 6–20 keV count rate for the four observations within 3 d (± 0.072 in orbital phase) of the periastron passage prior to the spin-up episode is 0.37 cm⁻² s⁻¹. The average rate for observations within 3 d of periastron, over the ASM lifetime, is 0.22 cm⁻² s⁻¹, with a standard deviation of 0.18 cm⁻² s⁻¹. Periastron rates comparable to those seen prior to spin up occur about every six orbits.

We constructed an average spectrum of all observations within 3 d of periastron ($\phi = 0.928 - 0.072$), and of observations in the same range of phases during the periastron passage prior to the spin-up episode, both shown in Figure 6. We fit both with a simple power law model with photoelectric absorption. The 90% confidence contours in photon index and normalization are shown in Figure 7. The best fit parameters of the average periastron passage are $A = 0.204(11)$ cm⁻²s⁻¹keV⁻¹ (at 1 keV), $\alpha = 0.924(19)$, and $n_H = 10^{23.61(09)}$. The spectral parameters of the periastron passage prior to the spin-up episode are $A = 1.1_{-0.8}^{+6}$ cm⁻²s⁻¹keV⁻¹ (at 1 keV), $\alpha = 1.2_{-0.4}^{+0.6}$, and $n_H = 10^{23.83(14)}$.

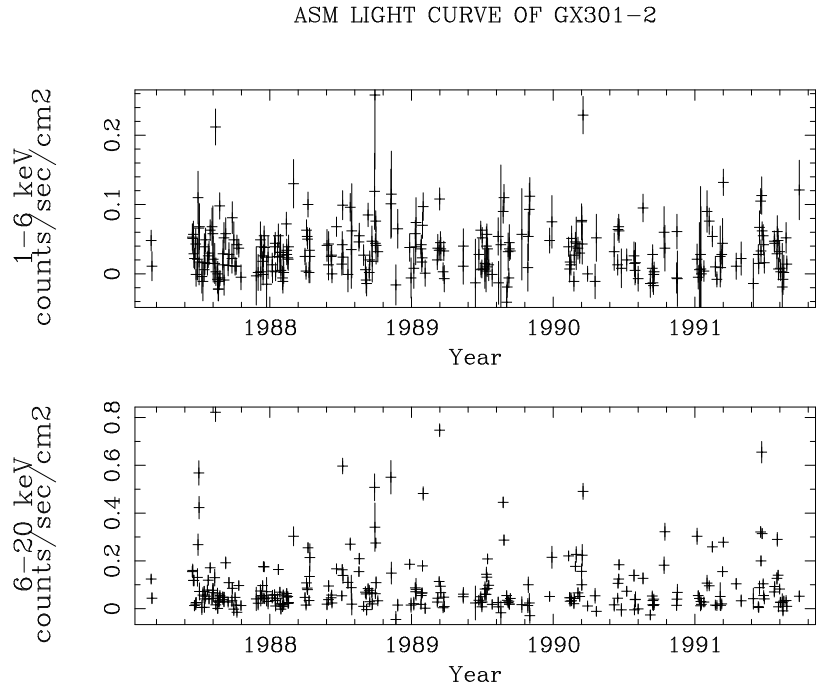


Fig. 5.— The 4.5 year flux history of GX 301-2 observed with *Ginga* ASM. Each data point corresponds to one scanning observation.

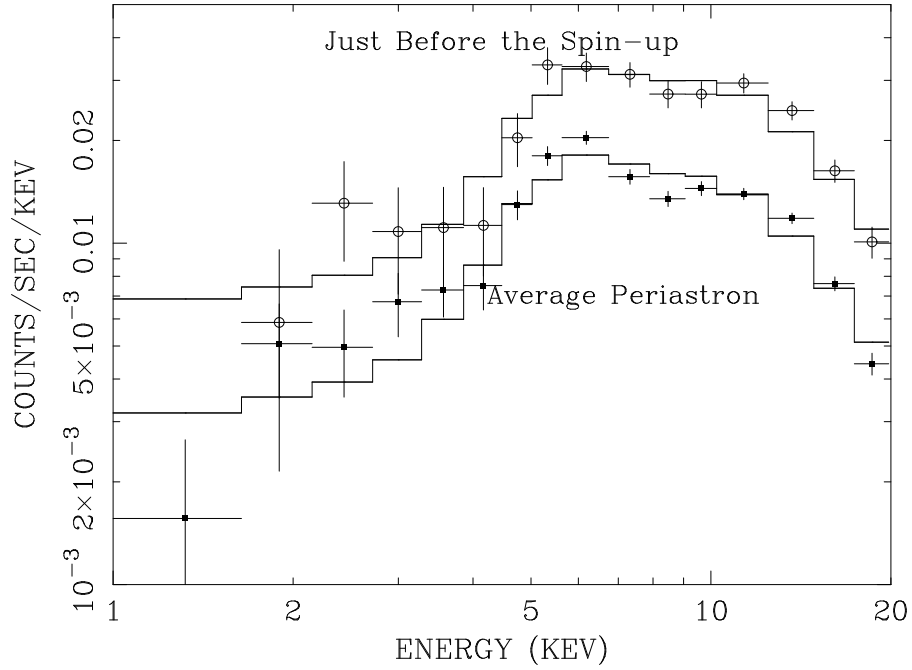


Fig. 6.— Two energy spectra of GX 301-2 obtained by *Ginga* ASM observations. Open circles indicate the average spectrum of four scans around the periastron passage (orbital phase 0 ± 0.072) just before the spin-up episode. The filled circles indicate the average spectrum in the corresponding orbital phase of all *Ginga* ASM data. The histograms are best fit power law models.

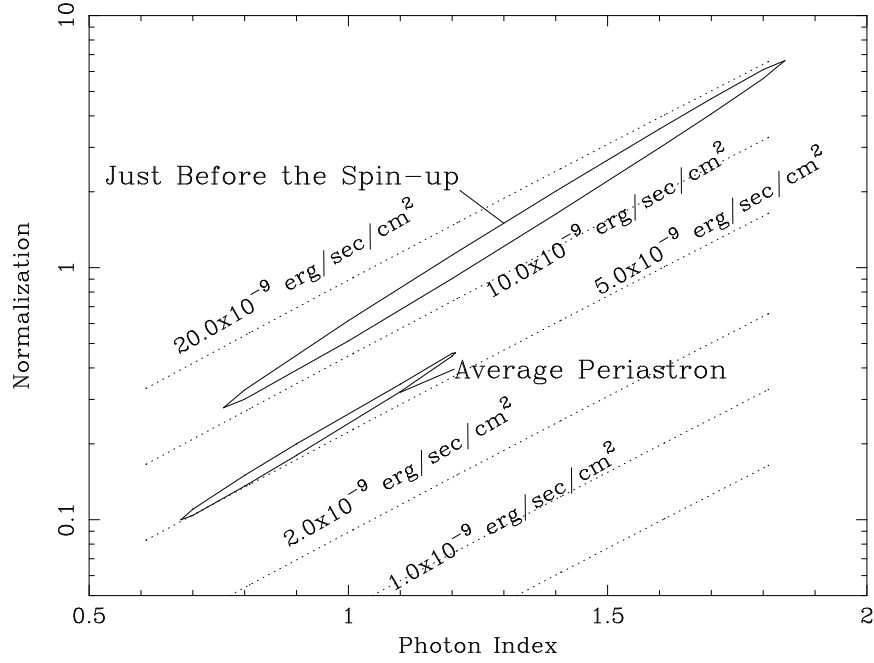


Fig. 7.— 90% confidence contours of the best parameters of spectral fitting for GX301-2. The dotted lines indicate constant flux levels.

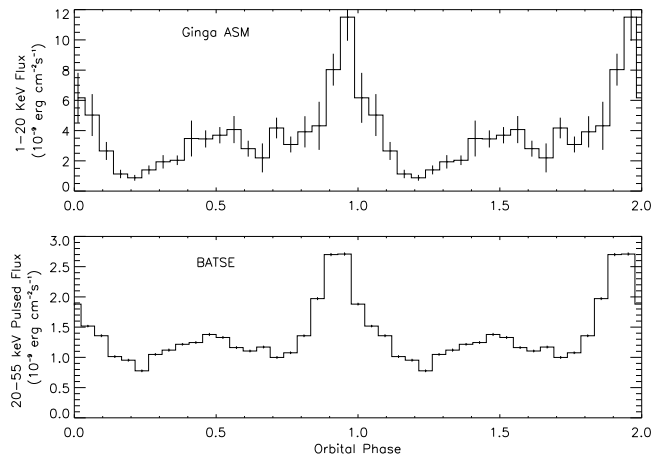


Fig. 8.— X-ray flux from GX 301-2 from the *Ginga* ASM (top panel) and BATSE (bottom panel, from Koh et al. 1997), as a function of orbital phase.

The spectral shape is consistent in the two fits. Lines of constant 6–20 keV flux are plotted in the figure, and the 1–20 keV and 6–20 keV fluxes are given in Table 2. Since X-rays below 6 keV are absorbed strongly, the uncertainty in 1–6 keV flux is large.

Figure 8 shows the *Ginga* ASM flux folded at an orbital period of $P_{\text{orb}} = 41.488$ d and referenced to an epoch of periastron of MJD 48,802.85 (Koh et al. 1997), along with the BATSE pulsed flux folded with the same orbit (Koh et al. 1997). The *Ginga* ASM fluxes were determined by folding ASM count rates corrected for effective area, then converting to a flux by assuming a constant spectral shape. The *Ginga* ASM and BATSE fluxes both show a peak shortly before periastron, a broad secondary maximum at apastron, and a minimum at orbital phase ~ 0.2 . The 1–20 keV flux is a factor of ~ 3 larger than the 20–55 keV pulsed flux, and shows amplitude modulations a factor of ~ 2 larger.

4. Discussion

Dynamical tests of accretion theory require simultaneous measurements of torque and bolometric luminosity. The observations presented here provide indirect evidence for a connection between accretion torque and luminosity in the persistent accreting pulsars 4U 1626–67 and GX 301–2.

The 1–20 keV flux is 20% lower in 4U 1626–67 during spin down than during spin up. No other single instrument observed the source in both states. It is notable that the 1–10 keV flux decreased by 55%, compared with a 20% change in the 1–20 keV flux. Measurements with the soft X-ray instruments ROSAT and ASCA during spin-down both yielded decreases of 60% or larger relative to the flux in the same band measured in 1979 with HEAO. The change in luminosity measured with the ASM is close to the 15% change in the magnitude of the accretion torque measured with BATSE. We now consider implications of our measurement to models of accretion torque. In the following discussion we will sometimes denote the spin frequency of the neutron star ν_* , rather than ν , to avoid confusion with other frequencies.

Pulsars cannot spin down while accreting in the simple picture of disk accretion outlined in §1. Near equilibrium, however, the accretion torque may depend in detail upon the disk-magnetosphere interaction. Spin-down can occur while material continues to accrete if negative, “non-material” torques are present. These may result from dragging of the magnetosphere by the disk outside the corotation radius, where the disk rotates more slowly than the neutron star (Ghosh & Lamb 1979). Alternatively, mass ejection in a magnetohydrodynamic wind may slow the neutron star (Arons & Lea 1980). Both models predict that a drop in \dot{M} causes a decrease in N , and potentially a reversal from spin up to spin down.

The model of Ghosh & Lamb is the most detailed. They derived a modified torque equation given

Table 2: GX 301-2 X-ray Flux

Bandpass	Spin-up Episode* 4 data in ± 3 days	Average Periastron* ± 3 days
1–20 keV	27.46 \pm 13.24	7.64 \pm 1.49
6–20 keV	15.11 \pm 3.94	5.60 \pm 0.52

* 10^{-9} erg cm $^{-2}$ s $^{-1}$

by $N = n(\omega)\dot{M}(GM_x r_m)^{1/2}$. The dimensionless function $n(\omega)$ is the same for all accreting pulsars. The “fastness” is defined as $\omega \equiv \nu_*/\nu_K(r_m)$, and is proportional to $\dot{M}^{-3/7}$. The function $n(\omega)$ increases smoothly with \dot{M} . It passes through zero at a critical value $\omega = \omega_c$, and approaches $n(\omega) = 1$ when $r_m \ll r_{co}$. Its exact form is somewhat controversial, but it is sufficient for our purposes that it can be written approximately as

$$n(\omega) \approx N_0 \left(\frac{1 - \omega/\omega_c}{1 - \omega} \right) \quad (5)$$

If the model of Ghosh and Lamb is correct, we can determine how close 4U 1626–67 is to equilibrium. In going from spin up to spin down, the change in accretion torque was $\delta N/N \sim -2$. Assuming $\dot{M} \propto L_x$, the change in \dot{M} was $\delta \dot{M}/\dot{M} = -0.2$. In general, $\delta\omega/\omega = -3/7(\delta\dot{M}/\dot{M})$ and $\delta N/N = (-\delta\omega/\omega_c)/(1 - \omega/\omega_c) + \delta\omega/(1 - \omega) + 6/7 \delta\dot{M}/\dot{M}$. Near equilibrium, where $\omega \approx \omega_c$ and $1 - \omega/\omega_c \ll 1 - \omega$, we have $\delta N/N \approx (\delta\omega/\omega)/(1 - \omega/\omega_c) + 6/7 \delta\dot{M}/\dot{M} = 3/7 (\delta\dot{M}/\dot{M})[1/(1 - \omega/\omega_c) + 2]$. From the measured $\delta\dot{M}/\dot{M}$ and $\delta N/N$ we find that during spin up, $w \approx 0.95 \omega_c$.

We can constrain the distance, D , to 4U 1626–67, from the luminosity and flux during spin up and from $\omega \approx 0.95 \omega_c$. Combining equations 1 and 3 and using $N = 2\pi I_x \dot{\nu}$ yields $2\pi I_x \dot{\nu} = r_x L_x (GM_x)^{-1/2} r_m^{1/2}$. Solving for r_m in terms of r_{co} and ω_c and using $r_{co}^3 = GM_x P_{spin}^2 / (4\pi^2)$ then gives us $L_x = (2\pi)^{4/3} (0.95\omega_c)^{-3/4} I_x \dot{\nu} r_x^{-1} (GM_x)^{1/3} P_{spin}^{-1/3}$. Finally, we assume that the 1–20 keV flux, F_x , is a fraction, $1/\eta$, of the bolometric flux. Using $\eta F_x = L_x / (4\pi D^2)$, and putting in the measured values of F_x , $\dot{\nu}$ and P_{spin} during spin up yields

$$\left(\frac{D}{5 \text{ kpc}} \right)^2 \left(\frac{r_x}{10 \text{ km}} \right) \left(\frac{M_x}{1.4 M_\odot} \right)^{-1/3} \left(\frac{I_x}{10^{45} \text{ g cm}^2} \right) = \frac{1}{\eta \sqrt{\omega_c}} \quad (6)$$

D must be at least ~ 5 kpc for a neutron-star with a mass of $1.4 M_\odot$, a radius of 10 km and a moment of inertia of 10^{45} g cm^2 . Chakrabarty et al. 1997a obtained a lower limit of 3 kpc using the higher flux value of $2.4 \times 10^9 \text{ ergs cm}^{-2} \text{ s}^{-1}$ measured with HEAO1 (Pravdo et al. 1979).

We can go on to determine ω_c if we further assume that the QPO observed in 4U 1626–67 during spin up is a magnetospheric beat-frequency oscillation satisfying $\nu_{QPO} = \nu_K(r_m) - \nu_*$ (Alpar & Shaham 1985; Lamb et al. 1985). By definition, $\omega = \nu_*/\nu_K(r_m)$. Substituting $\nu_K(r_m) = \nu_{QPO} - \nu_*$, with $\nu_* = 0.13 \text{ Hz}$ and $\nu_{QPO} = 0.04 \text{ Hz}$, and using $\omega = 0.95\omega_c$, yields $\omega_c = 0.8$. Equation (6) then yields a distance of ~ 5 kpc for η of order unity.

If $\nu_{QPO} = \nu_K(r_m) - \nu_*$, we would have expected ν_{QPO} to decrease in going from spin up to spin down. In fact the QPO frequency increased from 0.04 Hz to 0.048 Hz. One possible explanation is that $\nu_K(r_m)$ decreased from $\sim 0.17 \text{ Hz}$ to $\sim 0.08 \text{ Hz}$ and that ν_{QPO} changed from $\nu_K(r_m) - \nu_*$ to $\nu_* - \nu_K(r_m)$. This interpretation has two problems. First, it requires the magnetospheric radius to move outside the corotation radius. It is not known how accretion can occur when $r_m > r_{co}$. Second, the change in $\nu_K(r_m)$ then requires an approximately 80% decrease in \dot{M} . In contrast, we observed a 20% decrease in L_x . It is unlikely that the dependence of r_m on \dot{M} changes significantly near equilibrium since the magnetic energy density is a such strong function of radius ($B^2 \propto r^{-6}$). We think it more likely that the QPO in 4U 1626–67 is not a magnetospheric beat-frequency oscillation. If not, then we cannot estimate ω_c from these observations, and equation (6) provides only a lower limit to the distance.

A partial covering model provides a reasonable fit to the energy spectrum of 4U 1626–67 for 1990

June – 1991 October, with a 60% higher X-ray flux than 1987 April – 1990 June. Observationally, partial covering cannot be ruled out. However, the flux from 4U 1626–67 is low enough that even for a distance of 10 kpc the luminosity is substantially sub Eddington. We do not expect the physical conditions associated with partial absorption in wind-fed systems like as Vela X-1, such as an accretion wake, to be present.

In wind-fed systems small, transient accretion disks with frequent reversals in rotational sense are thought to form (e.g. Wang et al. 1981; Fryxell & Taam 1988). Wind-fed pulsars, such as Vela X-1 and GX 301–2, display erratic spin-frequency behavior that can be described as a random walk in spin frequency (Deeter & Boynton 1982; Bildsten et al. 1997). Because neither the rate nor the sense of accretion is constant, equilibrium is not a meaningful concept to apply to wind accretors. Correlations between torque and luminosity would have to be measured on the time scale of disk formation and reversal, which is thought to be of order hours to days.

The two episodes of steady spin up observed with BATSE in GX 301–2 were probably associated with the formation and accretion of a disk. During both episodes, the 20–55 keV pulsed flux was $\sim 50\%$ higher than average. However, since the average 1–20 keV flux is 3 times larger than the average 20–55 keV pulsed flux (see Figure 8), a change in spectral shape or pulsed fraction could have caused the enhancement seen by BATSE. The *Ginga* ASM did not observe GX 301–2 during the spin-up episode. However, the *Ginga* ASM flux, folded at the orbital period, is in good agreement with the BATSE pulsed flux folded with the same orbit. This agreement makes it unlikely that the increase of pulsed flux during the spin-up episode resulted just from a change in spectral shape or pulsed fraction, and strongly supports the correlation between luminosity and accretion torque inferred from the BATSE measurements. The flux enhancement seen with the *Ginga* ASM during the periastron passage prior to spin-up is further evidence for an increase in total flux during spinup. On the other hand, such an enhancement is seen in other periastron passages, and no such enhancement in the 20–55 keV pulsed flux is seen with BATSE during the periastron passage prior to spin up relative to other periastron passages.

Chichkov et al. see a periastron flare in the 1–20 keV flux with WATCH/GRANAT, along with evidence of flux enhancement at apastron and other phases. They measure an average peak periastron luminosity of $1.4 \times 10^{37} \text{ ergs s}^{-1}$ for a distance of $D = 1.8 \text{ kpc}$, a factor of 2 larger than the flux from the *Ginga* ASM. Their larger flux may be due to the harder spectral shape they assumed in converting from count rate to flux (White, Swank, & Holt 1983).

Our measurements provide indirect evidence for a connection between torque and luminosity in the persistent accreting pulsars 4U 1626–67 and GX 301–2. They reveal a $\sim 20\%$ change in the 1–20 keV X-ray flux of 4U 1626–67 between spin up and spin down, comparable to the change in $|\dot{\nu}|$. The ASM monitored 4U 1626–67 during the last 3 years of its extended spin up episode and during the first 16 months of spin down. The energy spectrum is significantly harder during spin down than during spin up – the change in the 1–10 keV flux is $\sim 50\%$. These observations highlight the importance of continuous, broad-band monitoring.

We confirm that the X-ray flux of GX 301–2 varies with orbital phase, as observed in 20–55 keV pulsed flux with BATSE. The shape of the 1–20 keV X-ray light curve shows all the features of the BATSE light curve. Although we do not observe the 1991 episode where BATSE observes an enhancement in the 20–55 keV pulsed flux accompanied by smooth, rapid spin up, the close similarity between the ASM and BATSE light curves indicate that the BATSE pulsed flux traces the bolometric flux, supporting the correlation between torque and luminosity suggested by the BATSE observations. The details of the connection between torque and luminosity in persistent pulsars remain unknown, and will require continued, simultaneous monitoring of the X-ray flux and spin frequency of these objects.

We wish to thank Robert Nelson, Danny Koh, and Deepto Chakrabarty for helpful comments and discussion. B.A.V. acknowledges support from the United States National Aeronautics and Space Administration under grants NAG5–3293 and NAG5–1458, and from the United States National Science Foundation under grant INT950–3950. This work was partially supported by Grant-in Aids from the Japanese Ministry of Education, Science, Sports and Culture (No. 09640320).

REFERENCES

- Alpar, M. A. & Shaham, J. 1985, *Nature*, 316, 239
- Angelini L., et al. 1995, *ApJ*, 449, L41
- Arons, J. & Lea, S. M. 1980, *ApJ*, 235, 1016
- Bildsten, L. et al. 1997, *ApJ*, submitted
- Chakrabarty, D. et al. 1997a, *ApJ*, 474, 414
- Chakrabarty, D. et al. 1997b, *ApJ*, 481, L101
- Chickhov, M. A., Sunyaev, R. A., Lund, I. Y., Brandt, S. & Castrotrirado, A. 1995 *Soviet Astron. Lett.*, 21, 435
- Davidson, K. & Ostriker, J. P. 1973, *ApJ*, 179, 585
- Deeter, J. & Boynton, P. 1982, *ApJ*, 261, 337
- Finger, M. H., Wilson, R. B., & Chakrabarty, D. 1996, *A&AS*, 120, C209
- Finger, M. H., Wilson, R. B., & Harmon, B. A. 1996, *ApJ*, 459, 288
- Fryxell, B. A. & Taam, R. E. 1988, *ApJ*, 335, 862
- Ghosh & Lamb 1979, *ApJ*, 234, 296
- Giacconi, R. et al. 1972, *ApJ*, 178, 281
- Koh, D. T. et al. 1997, *ApJ*, 479, 933
- Konigl, A. et al. 1991, *ApJ*, 370, L39
- Lamb, F. K., Shibazaki, N., Alpar, M. A., & Shaham, J. 1985, *Nature*, 317, 681
- Levine, A. et al. 1988, *ApJ*, 327, 732
- Middleditch, J. et al. 1981, *ApJ*, 244, 1001
- Nagase F. 1989, *PASJ*, 41, 1
- Parmar, A. N., White, N. E., & Stella, L. 1989a, *ApJ*, 338, 373
- Parmar, A. N., White, N. E., Stella, L., Izzo, C., & Ferri, P. 1989b, *ApJ*, 338, 359
- Pravdo, S. H. et al. 1979, *ApJ*, 231, 912
- Pringle, J. E. & Rees, M. J. 1972, *A&A*, 21, 1
- Reynolds, A. P., Parmar, A. N., Stollberg, M. T., Verbunt, F., Roche, P., Wilson, R. B., & Finger, M. H. 1996, *A&A*, 312, 872
- Shinoda K., Kii, T., Mitsuda, K., Nagase, F., Tanaka, Y., Makishima, K., & Shibazaki, N. 1990, *PASJ*, 42, L27.
- Tsunemi H., Kitamoto S., Manabe M., Miyamoto S., Yamashita K., and Nakagawa M., 1989, *PASJ*, 41, 391

- Tsunemi H., Kitamoto S. and Tamura K. 1996, *ApJ*, 456, 316
- Wang Y. M. 1981, *A&A*, 102, 36
- Warner, B. 1990, *Ap&SS*, 164, 79
- White, N. E., Swank, J. H., & Holt, S. S. 1983, *ApJ*, 270, 711
- Wilson, C. A., Finger, M. H., Harmon, B. A., Scott, D. M., Wilson, R. B., Bildsten, L., Chakrabarty, D., & Prince, T. A. 1997, *ApJ*, 479, 388